Available online at www.sciencedirect.com

ScienceDirect

Procedia Engineering 207 (2017) 1475–1480

Procedia Engineering

www.elsevier.com/locate/procedia

International Conference on the Technology of Plasticity, ICTP 2017, 17-22 September 2017, Cambridge, United Kingdom

Effect of severe plastic deformation and post-annealing on the mechanical properties and bio-corrosion rate of AZ31 magnesium alloy

Bryan Shi Jie Bin[a]; Yong Teck Tan[b]; Kai Soon Fong[b*]; Ming Jen Tan[c]

[a] School of Material Science and Engineering, Nanyang Technological University, 11 Faculty Ave, Singapore 6399772
[b] *Singapore Institute of Manufacturing Technology, 73 Nanyang Drive, Singapore 637662*
[c] *School of Mechanical and Aerospace Engineering, Nanyang Technological University, 50 Nanyang Avenue, Singapore 639798*

Abstract

In this work, the effect of fine grain sizes on the mechanical and bio-corrosion properties of AZ31 magnesium alloy was studied. Bio-corrosion refers to the accelerated degradation of metal within the human body. Fine-grained (~1.5 μm) AZ31 was obtained through Severe Plastic Deformation (SPD) via three cycles of Constrained Groove-Pressing (CGP) under elevated temperature. The effects of CGP and post-annealing (at 473 K for 15 and 30 min) on bio-corrosion were preliminarily investigated by potentiodynamic polarization measurements and constant immersion tests. Results obtained show that the as-processed samples with annealing exhibited improvements in yield strength and ductility while the bio-corrosion rate in Hank's solution remains fairly similar during the early stage.

Peer-review under responsibility of the scientific committee of the International Conference on the Technology of Plasticity.

Keywords: Severe Plastic Deformation ; Corrosion; Magnesium ; AZ31

* Corresponding author. Tel.: +65 6793 8974;
E-mail address: ksfong@simtech.a-star.edu.sg

1877-7058
Peer-review under responsibility of the scientific committee of the International Conference on the Technology of Plasticity.
10.1016/j.proeng.2017.10.916

1. Introduction

Magnesium alloys are gaining importance in the field of biomedical engineering, especially in the aspect of orthopedics as a metallic biomaterial. Current metals used as biomaterials include titanium and stainless steels, which have high corrosion resistance coupled with good mechanical strength and fracture toughness [1]. However, limitations such as the release of toxic ions [2] and particularly, stress shielding effect due to the mismatch of elastic moduli can promote instability in the implant and impede bone growth *in vivo* [3].

Magnesium and its alloys on the other hand, is a remarkably lightweight material (density of 1.74 g/cm^3) that is three times less dense compared to titanium. Unlike current metallic biomaterials, oxidation of magnesium promotes magnesium ions, which is essential to the metabolism of a human body and secretion of insulin, aiding in the healing process of the bone [5]. It also prevents the need for a second surgery to remove implant that can cause discomfort to the patient. More importantly, the elastic modulus as well as the yield strength of magnesium is closer to that of natural bone, which aids in the stimulation of bone growth. However, the high corrosion rate of magnesium alloys and the dissolution of) hydrogen gas beneath the skin are major concerns in developing magnesium implants [4].

Alloying is an important process that can increase magnesium alloy's corrosion resistance, further enhanced by surface treatment and coating [4,6-7]. However, alloying elements, surface treatment and coating are limited in the application of biomedical engineering as it is essential that any additives must be non-toxic. AZ31 was proposed in this experiment because the presence of 3 wt. % of Al resulted in optimum corrosion resistance. On the other hand, addition of more Al above 3 wt. % led to a drop in corrosion resistance [6]. Recent studies have shown that microstructure refinement is another alternative that can improve corrosion resistance without using additives. Microstructural features such as the formation of a compact $Mg(OH)_2$ film prevents further attack on the metal thereby improving corrosion resistance [7]. However, there are opposing arguments presented which suggest that fine-grain sizes tend to have higher corrosion rate due to the presence of localized corrosion. Localized corrosion occurs due the formation of secondary phase precipitate at the grain boundary. These secondary phase precipitate are generally more active compared to the matrix, thus making the grain boundary anodic relative to the bulk, thereby causing corrosion. [8]. However, it is debatable if magnesium alloys suffer from this type of corrosion as localized corrosion in magnesium starts as irregular pits that spreads laterally instead of forming deep pits as discussed by Song and Atrens [13]. In addition, grain boundaries are high energy sites where corrosion is preferentially initiated at. Smaller grain size give rise to higher fraction of grain boundary thus increasing corrosion rate [8]. While smaller grain size promotes shielding of α phase by the β phase that results in improved corrosion resistance, the smaller grain size also increases the fraction of grain boundary, which promotes anodic oxidation. Therefore, there is a need to identify a clear relationship between grain size and corrosion resistance of AZ31.

2. Experimental procedure

2.1. Material

Plates of size 96 mm x 96 mm with 2 mm thickness of wrought AZ31 magnesium alloy of composition (in wt. %): 2.4 % Al-0.85 % Zn-0.98 %-balance Mg were used and processed by three cycles of constrained groove pressing (CGP) at elevated temperature to achieve fine grain sizes. The deformation temperature was maintained at 503±2 K in the first cycle and 453±2 K in the last two cycles. In each cycle, the plate was pressed four times (with a 90° rotation of the plate after each press) between a pair of groove die and straightened by pressing between a pair of flat die in the last step. During each pressing, the plate was placed onto the lower die and heated for 2 minutes. After each pressing, the plate was removed from the die to cool in air. The design of the groove die has an angle of 45° and pitch of 8 mm. Samples of size 10 mm ×10 mm and 20 mm × 20 mm were cut from the central part of the plate for immersion test and electrochemical measurements respectively. The initial and as-processed material are referred to as as-received and CGP samples, respectively. Annealing of the CGP samples were also carried out at 473 K for 15 and 30 minutes, and are referred to as CGP-15 and CGP-30 samples respectively.

2.2. Tensile Tests

Specimens for tensile testing were cut along the rolling direction of the plate into a gauge length of 25 mm x 6 mm x 1.5 mm, in accordance to ASTM E8M Standard. Tensile tests were conducted with an initial strain rate of 3 x 10^{-3} s^{-1}. The 0.2% offset yield stress was taken from the engineering stress-strain curve and elongation to failure was taken at engineering strain at fracture.

2.3. Corrosion Tests

Electrochemical tests were conducted using a potentiostat and a standard three-electrode system in an electrochemical test cell with Hank's solution as the electrolyte. Hank's solution is a solution made to a physiological pH and salt concentration which simulates body fluid with a pH of 7.3 and at a constant temperature of 37.5°C. The counter electrode was a high-density graphite rod; reference electrode was a saturated calomel electrode (SCE); and the working electrode was the metal specimen, covered with an electrochemical mask exposing an area of 1 cm^2. The open circuit potential (OCP) was measured for one hour before potentiodynamic polarization was conducted at a scan rate of 1 mV/s. Tafel fitting was used to obtain the corrosion current density (i_{corr}) from the polarization scan. Each sample condition was measured three times to ensure the consistency of results obtained.

Immersion tests were conducted where samples were polished with SiC paper up to 1200 grit, cleaned ultrasonically with acetone and dried under compressed air. Four specimens were each placed in separate beakers containing Hank's solution at a constant temperature of 37.5°C, where the volume of Hank's solution was maintained at 6.7 times of the total surface area of each sample across the duration of immersion experiment [4]. Immersion studies were carried out for 24 h, 48 h and 168 h where the weights of all specimens were measured before and after each immersion test. The samples were taken out after each time interval where they were rinsed with de-ionized water and air-dried before immersing in chromic acid solution of concentration 200 g/dm^3 to remove any corrosion products. Samples were then air-dried before measuring the weight loss. Two repeats of corrosion rate is then calculated by [4]:

$$\text{Corrosion rate (mm/year)} = \frac{\Delta \boldsymbol{w} \times \boldsymbol{k}}{\boldsymbol{A} \times \boldsymbol{t} \times \boldsymbol{\rho}} \quad (1)$$

Where $\Delta \boldsymbol{w}$ is the weight loss, g; constant, $\boldsymbol{k}$ = 87600; $\boldsymbol{A}$ is the total surface area exposed to Hank's Solution, cm^2; $\boldsymbol{t}$ is the time of immersion in Hank's Solution, hr.; $\boldsymbol{\rho}$ is the density of the material immersed in Hank's solution.

3. Results and Discussion

3.1 Microstructure observations and mechanical properties

Fig. 1 shows the microstructures observed on the surface of the samples. The samples' average grain sizes and mechanical properties are summarized in Table 1 and Fig. 2, respectively. Through CGP processing, the yield strength was enhanced by ~39% from 175 MPa to 243 MPa. However, this was achieved at the expense of ductility which dropped significantly by ~90% from 19% to 2%. This improvement in yield strength is attributed to the fine-grained structure and strain hardening after CGP, while the loss in ductility is due to the plastic strain instability caused by the decrease in strain hardening ability of the fine-grained material [10]. Annealing treatments were able to recover this loss in ductility (17-22%) to equal or better than the as-received sample albeit some decrease in yield strength (206-216 MPa). Even so, the yield strength is still ~18-20% higher than the as-received sample. Ideally, the bio-metallic material should have high yield strength and fatigue strength to resist fracture due to cyclic loading. Sufficient ductility (~8%) should also be retained so that further contouring or shaping of the material into potential applications, such as fixation screws and plates can be made. Therefore, optimum-annealing condition should be carefully explored in the future

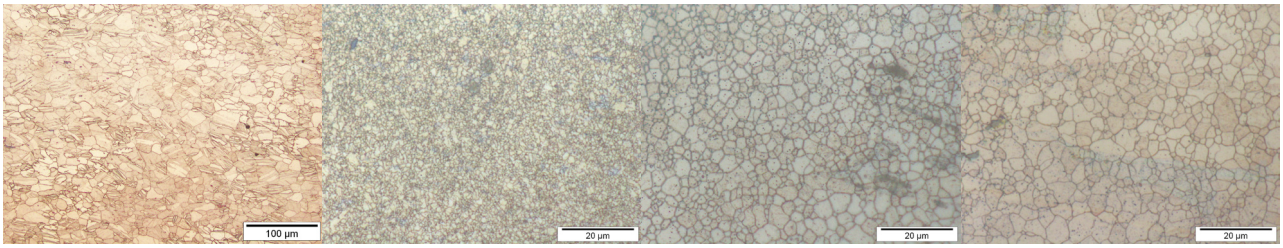

Fig. 1. Optical micrographs of the different samples; (a) as-received, (b) as-processed (CGP), (c) CGP annealed at 473 K for 15 min (CGP-15) and (d) CGP annealed at 473 K for 30 min (CGP-30).

Table 1. Average grain sizes for different sample conditions.

	Average grain size (µm)	Standard deviation (µm)
Initial material (as-received)	15.0	0.7
As-processed through CGP (CGP)	1.6	1.4
CGP and annealed at 473 K for 15 min (CGP-15)	3.4	1.7
CGP and annealed at 473 K for 30 min (CGP-30)	4.8	1.5

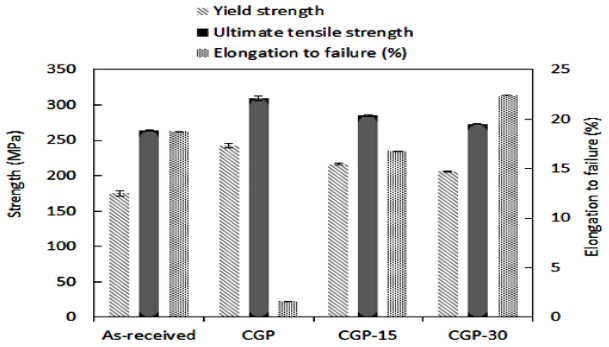

Fig. 2. Mechanical properties measured from tensile tests in the rolling direction.

3.2 Electrochemical test analysis

According to the mixed potential theory by Wagner and Traud [12], the sum of currents from anodic reactions (oxidation processes) must be equal to the sum of currents from cathodic reactions (reduction processes) for an electrode under open-circuit conditions. The potential that this situation occurs is called the corrosion potential (E_{corr}). At E_{corr}, the anodic current density is equal to the cathodic current density, resulting in a net current density of zero. The anodic current density at E_{corr} is the corrosion current density (i_{corr}) and is a direct measure of the corrosion rate (higher i_{corr} indicating a higher corrosion rate). Therefore, to measure the corrosion rate of a metal, Tafel fitting of the anodic and cathodic branches of its polarisation curve can be done to obtain the i_{corr} value. The set of simplified equations below give the chemical reactions occurring during the corrosion process:

$$\text{Anodic reaction : } Mg_{(s)} \rightarrow Mg^{2+}_{(aq)} + 2\,e^-$$

$$\text{Cathodic reaction : } 2H_2O_{(l)} + 2\,e^- \rightarrow H_{2\,(g)} + 2\,OH^-_{(aq)}$$

$$\text{Overall: } Mg_{(s)} + 2H_2O_{(l)} \rightarrow Mg^{2+}_{(aq)} + H_{2\,(g)} + 2\,OH^-_{(aq)}$$

Fig. 3 shows the potentiodynamic polarization curves for the four samples. The average i_{corr} values were 7.8±0.8 x 10^{-6} A/cm^2, 1.5±0.7 x 10^{-5} A/cm^2, 2.0±0.8 x 10^{-5} A/cm^2 and 1.0±0.6 x 10^{-5} A/cm^2 for the as-received, CGP, CGP-15, and CGP-30 samples. These results indicate that the as-received sample has better corrosion resistance, although these values are relatively close to each other within the limits of experimental error.

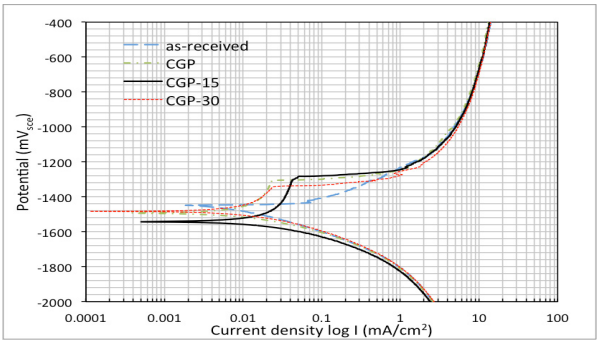

Fig. 3. Potentiodynamic polarization curves for different samples.

Although electrochemical techniques are widely used to measure the corrosion rate of metals, it may not be the most suitable measurement technique for magnesium. Research by Song and Atrens [13, 14] and Frankel et al. [15] indicates that the hydrogen evolution rate continues to increase even above the corrosion potential, contrary to standard electrochemical kinetics theory. This continued hydrogen evolution on the Mg surface consumes electrons that would have otherwise flowed through the potentiostat, resulting in an underestimation of the corrosion rate. Therefore, weight loss measurement was conducted up to 168 hours as an alternative technique for corrosion rate measurement to supplement the data obtained from the polarization experiments.

3.3 Immersion tests

The results of the immersion tests are given in Fig. 4 as a plot of corrosion rate against time immersed in Hank's solution. Up to 48 hours, the corrosion rate of the different samples were relatively similar within the limits of experimental error. Note that the electrochemical results from the polarization experiments (after 1 hour immersion) are in agreement with the immersion test results at 24 hours. Both techniques indicate that the corrosion rate of as-received and of as-processed samples (with and without annealing) are fairly similar at the beginning.

However, after 168 hours of immersion, the as-processed conditions (with and without annealing) generally had a higher corrosion rate compared to the as-received samples. This property of higher corrosion rate at later stages may be exploited for suitable applications. More studies will be conducted in future to determine the cause of this phenomenon. No clear trend was observed in this work between the corrosion rate and the grain size. The corrosion rate at early times (24 hours up to 48 hours) was roughly the same despite the different grain sizes (Table 1). At later times (168 hours), the as-received samples (largest average grain sizes) had the lowest corrosion rate (Fig. 4) but the CGP-30 samples having the second largest average grain sizes had the highest corrosion rate while the CGP samples having the smallest grain sizes had the second lowest corrosion rate. Hence more studies are also required to clarify the trend between grain size and corrosion rate.

The main inference here is that the thermomechanical processing did not have a significant effect on the early stage corrosion resistance of AZ31 magnesium alloy although it may have an effect at later stages. More work has to be done to determine the optimal heat treatments that would improve corrosion resistance by varying heat treatment time and temperature. Microstructure characteristics such as dislocation density effect on corrosion should also be examined.

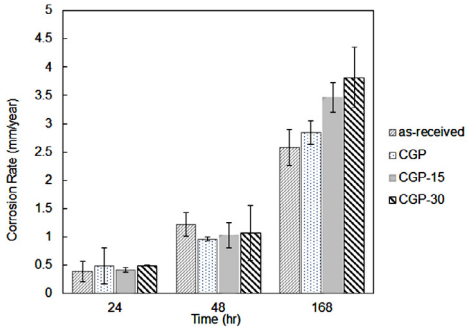

Fig. 4. Corrosion rate of as-received and as-processed AZ31 in Hank's solution as a function of time.

4. Conclusion

(1) Thermomechanical treatments by constrained groove pressing and annealing were utilised to achieve fine grain microstructure (1.5 μm – 5 μm) in comparison with as-received sample (15 μm).
(2) Potentiodynamic polarisation experiments and constant immersion tests indicate that the corrosion rate of as-received and of as-processed specimens (with and without annealing) are similar in the early stage. However, at later stages, the corrosion rate of the as-processed specimens (with and without annealing) were higher than the as-received samples.
(3) No clear trend was observed between the corrosion rate and grain size for AZ31 alloy in this study.

Acknowledgment

We wish to acknowledge the funding for this project from Nanyang Technological University under the Undergraduate Research Experience on CAmpus (URECA) programme and A*STAR Singapore Institute of Manufacturing Technology (SIMTech).

References

[1] Ye, X., Tse, Z. T. H., Tang, G., Song, G.. Mechanical properties and phase transition of biomedical titanium alloy strips with initial quasi-single phase state under high-energy electropulses, Journal of the Mechanical Behavior of Biomedical Materials 42 (2015) 100–115.
[2] Puleo, D. A., Huh, W. W.. Acute toxicity of metal ions in cultures of osteogenic cells derived from bone marrow stromal cells, Journal of Applied Biomaterials : An Official Journal of the Society for Biomaterials 6(2) (1995) 109–116.
[3] Nagels, J., Stokdijk, M., Rozing, P. M.. Stress shielding and bone resorption in shoulder arthroplasty, Journal of Shoulder and Elbow Surgery (2003).
[4] Yang, L., Zhang, E.. Biocorrosion behavior of magnesium alloy in different simulated fluids for biomedical application, Materials Science and Engineering C. 29(5) (2009) 1691–1696.
[5] Gray, J. E., Luan, B.. Protective coatings on magnesium and its alloys — a critical review, Journal of Alloys and Compounds 336 (2002) 88–113.
[6] Homayun, B., Afshar, A.. Microstructure, mechanical properties, corrosion behavior and cytotoxicity of Mg-Zn-Al-Ca alloys as biodegradable materials, Journal of Alloys and Compounds 607 (2014) 1–10.
[7] Song, Y., Shan, D., Chen, R., Zhang, F., & Han, E. H. Biodegradable behaviors of AZ31 magnesium alloy in simulated body fluid. Materials Science and Engineering C, 29(3) (2009) 1039–1045.
[8] Song, D., Ma, A., Jiang, J., Lin, P., Yang, D., & Fan, J.. Corrosion behavior of equal-channel-angular-pressed pure magnesium in NaCl aqueous solution. Corrosion Science, 52(2) (2010) 481–490.
[9] Witte, F., Hort, N., Vogt, C., Cohen, S., Kainer, K. U., Willumeit, R., Feyerabend, F.. Degradable biomaterials based on magnesium corrosion, Current Opinion in Solid State and Materials Science. 12(5–6) (2008) 63–72.
[10] Ovid'ko, I.A., Langdon, T.G.. Enhanced ductility of nanocrystalline and ultrafine-grained metals, Review on Advanced Materials Science (2012) 103-111.
[11] Witte, F.. Reprint of: The history of biodegradable magnesium implants: A review, Acta Biomaterialia 23 (2015) 28–40.
[12] Wagner, C., Traud, W.. Über die deutung von korrosion vorgangen durch uber- lagerung von elektrochemischen teilvorgangen und uber die potentialbildung an mischellektroden, Zeitschrift Fur Elektrochemie 44 (1938) 391–402.
[13] Song, G., Atrens, A.. Understanding Magnesium Corrosion—A Framework for Improved Alloy Performance, Advanced Engineering Materials 5(12) (2003) 837–858.
[14] Shi, Z., Liu, M., Atrens, A.. Measurement of the corrosion rate of magnesium alloys using Tafel extrapolation, Corrosion Science 52(2) (2010) 579–588.
[15] Frankel, G.S., Samaniego, A., Birbilis, N.. Evolution of hydrogen at dissolving magnesium surfaces, Corrosion Science 70 (2013) 104–111.